

---

# What Happens During the Loss Plateau? Understanding Abrupt Learning in Transformers

---

**Pulkit Gopalani**

University of Michigan, Ann Arbor  
gopalani@umich.edu

**Wei Hu**

University of Michigan, Ann Arbor  
vvh@umich.edu

## Abstract

Training Transformers on algorithmic tasks frequently demonstrates an intriguing *abrupt learning* phenomenon: an extended performance plateau followed by a sudden, sharp improvement. This work investigates the underlying mechanisms for such dynamics, primarily in shallow Transformers. We reveal that during the plateau, the model often develops an interpretable *partial solution* while simultaneously exhibiting a strong *repetition bias* in their outputs. This output degeneracy is accompanied by *internal representation collapse*, where hidden states across different tokens become nearly parallel. We further identify the slow learning of optimal attention maps as a key bottleneck. Hidden progress in attention configuration during the plateau precedes the eventual rapid convergence, and directly intervening on attention significantly alters plateau duration and the severity of repetition bias and representational collapse. We validate that these identified phenomena—repetition bias and representation collapse—are not artifacts of toy setups but also manifest in the early pre-training stage of large language models like Pythia and OLMo.

⌚ [github.com/pulkitgopalani/tf-loss-plateau](https://github.com/pulkitgopalani/tf-loss-plateau)

## 1 Introduction

Training Transformers on mathematical or algorithmic tasks often exhibits an intriguing “abrupt learning” phenomenon in their training dynamics, where the model’s performance plateaus at a suboptimal level for an extended period before suddenly and rapidly converging to the optimal solution [30, 2, 37, 46, 39] (Figures 1 and 2). This is often considered an example of the broader phenomenon of “emergence,” where model capabilities appear to arise discontinuously and unpredictably with increasing amount of parameters, training data, or training steps [41]. Understanding these sharp phase transitions in learning trajectories is crucial for gaining deeper insights into how Transformer models learn and develop their sophisticated capabilities.

Despite recent progress in understanding such abrupt learning dynamics in Transformers for specific tasks like in-context learning [37, 46, 39, 8, 34], parity learning [2], Markov chains [12], grammar learning [27], and matrix completion [15], a unifying account of the model evolution during loss plateau is still missing. Further, many of these works require specific assumptions on model and data that limit their generality.

The goal of this paper is to uncover universal characteristics and underlying mechanisms that define these training dynamics that are broadly applicable to a wide range of setups and tasks. Specifically, what common patterns manifest in the model’s input-output behavior and internal representations during the extended plateau phase, and what critical changes precede the sudden shift towards higher performance? Is there hidden progress accumulating beneath the surface of the loss plateau? Answering these questions is pivotal for building a comprehensive picture of the nature of phase transitions in Transformer training dynamics.

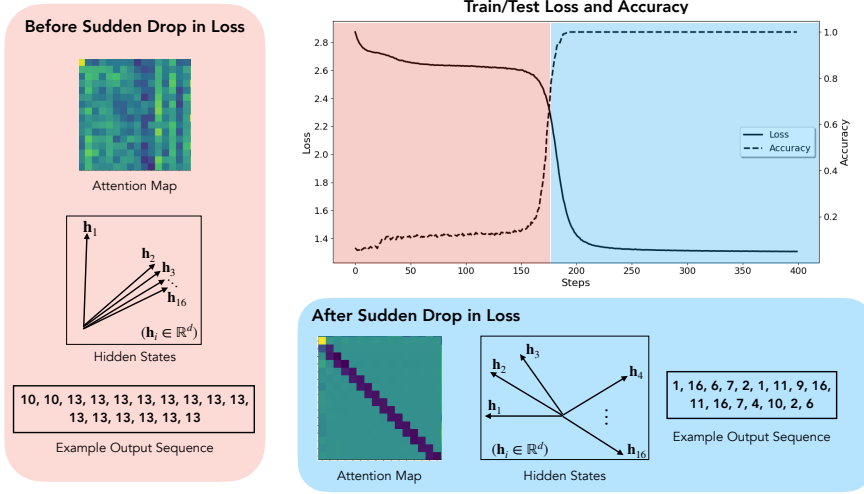


Figure 1: **Abrupt learning and related characteristics.** Training a shallow Transformer on algorithmic tasks like moving-window-sum exhibits an *abrupt learning* curve: performance plateaus for an extended number of steps, before suddenly and sharply improving to optimum. Before the sudden drop in loss, the attention map cannot be interpreted easily, whereas the post-sudden-drop attention map is clearly interpretable w.r.t. the task. Furthermore, the model exhibits degenerate patterns before the sudden drop, including output repetitions and collapse of its hidden representations.

To investigate these questions systematically and within a controlled setting, we focus on training small, shallow Transformers (typically 1 or 2 layers) on a suite of simple algorithmic tasks. The reduced model size allows for more tractable analysis and clearer interpretation of internal model mechanisms, avoiding the obfuscation that can arise from the interplay of countless factors in large models. Furthermore, algorithmic tasks such as moving-window-sum, prefix-sum, and multi-digit addition (as detailed later) have well-defined optimal solutions, thus allowing us to precisely measure the model’s progress against a known ground truth and to readily interpret which aspects of the problem the model is succeeding on at different training stages. Interestingly, we will demonstrate that key findings from these controlled small-scale studies extend to the pre-training dynamics of actual Large Language Models (LLMs).

**Our Contributions.** We identify novel implicit biases that underlie the early plateau period of Transformer training: the model learns a partial solution while being biased toward degenerate patterns in its outputs and internal representations. We further study the pivotal role of attention map learning in driving these phenomena and overcoming the performance plateau. See Figure 1 for an overview of our findings. Our specific contributions are:

- **Partial solutions during plateau:** We show that during the initial loss plateau, the model often learns a **partial solution**, which correctly predicts a subset of easier tokens within a sequence—those that might be intuitively simpler to learn (e.g., copying the first element in a moving-window sum, or predicting the final carry-over in multi-digit addition)—while failing on more complex parts of the task. This pattern is observed across diverse algorithmic tasks (Table 1).
- **Repetition bias in outputs:** We identify a strong **repetition bias** during the plateau, where the model tends to output repetitive tokens. This bias can be quantified by metrics such as a direct count of repeated subsequent tokens or the entropy of the output token distribution. Such repetitions significantly increase during the early training steps and then markedly decrease as the performance starts to improve (Figure 2b).
- **Internal representation collapse:** The output repetition bias is accompanied by **representation collapse**, where hidden representations for different tokens become nearly parallel (e.g., cosine similarity often exceeds 0.9), indicating a degenerate representational geometry inside Transformers. Subsequently, this representational similarity drops significantly as the model’s performance improves, signifying a diversification of internal representations (Figure 2b).

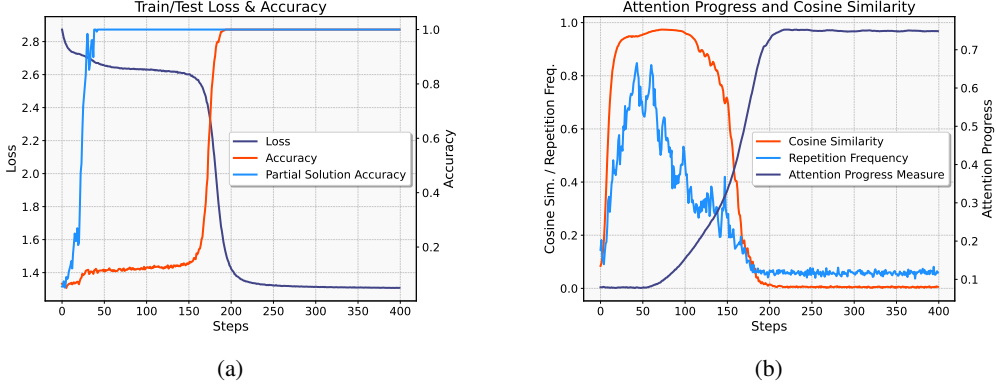


Figure 2: **Abrupt learning dynamics for the MWS task.** (a): Train/Test loss and Train/Test Accuracy (note that both train and test data metrics are near-identical in the online training setup, and thus we only report train metrics); (b): Attention Progress, Repetition Frequency, and Representation Cosine Similarity between hidden states. Increase in attention progress is gradual and happens before the sudden loss drop. Repetition frequency and representation cosine similarity rapidly increase at the beginning and decrease to low values later on.

- **Crucial role of attention map learning:** We find that gradual learning of the optimal attention pattern can commence during the loss plateau, before the sudden drop in loss (Figure 2b). By directly intervening on the attention map during training—for instance, by biasing the attention scores towards or away from the optimal configuration—we can observe tangible changes in the duration of loss plateau and the severity of degenerate behaviors like repetition bias and representation collapse.
- **Validation in LLMs:** Our identified phenomena of repetition bias and representation collapse are not limited to small Transformers on synthetic algorithmic tasks. We further validate their occurrence in the early pre-training phases of LLMs like Pythia and OLMo, suggesting these are general characteristics of Transformer training dynamics.

## 2 Setup, Abrupt Learning, and Attention Map

We mainly present results for the moving-window-sum task in the main text, which we define below; we also validate our findings on various other algorithmic tasks like multi-digit addition, permutations, histogram, prefix-sum, etc., in Appendix B.

**Data.** The moving-window-sum (MWS) task involves computing the sliding-window sum (modulo  $p$ ) of a length- $n$  sequence over windows of size 2; that is, sequences in MWS are

$$x_1, x_2, \dots, x_n, \text{SEP}, y_1, y_2, \dots, y_n$$

$$y_i = \begin{cases} x_1 & i = 1 \\ (x_{i-1} + x_i) \bmod p & i \geq 2 \end{cases}$$

Here,  $x_1, \dots, x_n$  are the input sequence, SEP is a separator token, and the task is to complete the sequence with outputs  $y_1, \dots, y_n$ . In the experiments in the main paper, we use  $n = 16$ ,  $p = 17$ ,  $x_i \sim \text{Unif}\{1, 2, \dots, 16\}$  and  $\text{SEP} = 17$ . We denote the full vocabulary  $V := \{0, 1, 2, \dots, 17\}$ .

**Model Architecture.** We use a 1-layer, 1-head Transformer with causal masking and linear attention. This simple architecture can already solve the MWS task to perfect accuracy. Formally, for a sequence of tokens  $(s_1, \dots, s_L)$ , the Transformer output is,

$$\text{TF}_\theta(s_1, s_2, \dots, s_L) = \text{LM} \circ (\text{Id} + \text{MLP}) \circ (\text{Id} + \text{Attn}) \circ \text{Embed}(s_1, s_2, \dots, s_L)$$

where  $\text{Embed}$  outputs sum of token and absolute positional embeddings  $h_i \in \mathbb{R}^d$ , and  $\text{Attn}$  denotes the causal-linear-Attention operation that combines tokens such that output at  $i^{\text{th}}$  position is,

$$[\text{Attn}(h_1, h_2, \dots, h_L)]_i = W_O \left( \sum_{j=1}^i (h_j^\top W_K^\top W_Q h_i) W_V h_j \right); \quad W_O, W_K, W_Q, W_V \in \mathbb{R}^{d \times d}.$$

MLP denotes the 2-layer neural net  $h_i \mapsto W_2(\sigma(W_1 h_i))$  for  $W_2 \in \mathbb{R}^{d \times 4d}$ ,  $W_1 \in \mathbb{R}^{4d \times d}$ , and  $\sigma$  the GELU activation. LM is a linear layer that maps the hidden state  $h_i \in \mathbb{R}^d$  to logits  $v_i \in \mathbb{R}^{|V|}$ . Note that all linear maps above implicitly include a bias term, and we use pre-LayerNorm so that before the Attn, MLP, and LM, a LayerNorm operation is applied to the hidden states  $h_i$ . For generating sequences, we use greedy decoding i.e. output token is determined by the maximum logit over the vocabulary (please see Appendix A for more implementation details). We use linear attention to avoid vanishing gradient issues from softmax attention being a contributing factor toward abrupt learning, which was argued in [17]. We also show similar results on softmax attention, multi-layer / multi-head models, and models with varying  $d$  in Appendix D.

**Training.** The model is trained to minimize the standard next-token-prediction cross-entropy loss over the full sequence i.e.  $(x_1, \dots, x_n, \text{SEP}, y_1, \dots, y_n)$  for the MWS task. We evaluate accuracy over the output portion of the sequence, i.e.,  $y_1, \dots, y_n$ , averaged over these  $n$  positions. We use the Adam optimizer with a constant learning rate  $10^{-4}$  and no weight decay. The training is conducted in an online / single-epoch fashion, where a new batch of 256 training samples is drawn from the data distribution at each training step. Note that in this setup, the training and test losses essentially coincide. For completeness, we also show similar results on the SGD optimizer in Appendix D.

**Abrupt Learning.** Following the training procedure described above will result in a characteristic *abrupt learning* curve, where the training/test loss is stuck at some sub-optimal value for a significant number of steps, before suddenly and rapidly decreasing to its optimal value (Figure 2a). This drop in loss is accompanied by a similarly rapid increase in accuracy, indicating that the optimal solution is learned abruptly.

**Attention Map.** We analyze the attention map at different points during training. We find that the attention map shows a sparse, interpretable pattern after the sudden loss drop, while no such pattern is shown before the sudden drop (Figure 1). For the MWS task, this optimal attention pattern corresponds to each output token  $y_i$  attending only to the input tokens relevant to its computation, i.e., attending to  $x_1$  for  $y_1$ , and to  $x_i, x_{i-1}$  for  $y_i, i \geq 2$ . We further use an *Attention Progress Measure (APM)* to record the progress of the attention map toward its optimal pattern during training, defined as

$$\text{APM} := \frac{\sum_{(i,j) \in \Omega} |A_{ij}|}{\sum_{(i,j)} |A_{ij}|},$$

where  $A_{ij}$  denotes the attention score allocated to the  $j^{th}$  token when computing output at the  $i^{th}$  position in the sequence, and  $\Omega$  is the set of position pairs in the optimal attention map. This measure is defined with absolute values due to our choice of linear attention so that  $A_{ij}$  could be positive or negative. In experiments, we calculate APM averaged over a random batch of sequences.

Figure 2b shows that the APM monotonically increases from near 0 to near 0.8 during training, and its increase is more gradual than the loss/accuracy dynamics. In particular, APM already increases to a nontrivial value during the loss plateau and before the sudden loss drop.

### 3 Implicit Biases in the Early Phase of Training

In this section, we characterize several key manifestations of the implicit biases in the early phase of Transformer training. These patterns robustly co-occur with the loss plateau, and provide intuitive indicators that the model is getting stuck at a degenerate state during the plateau.

**Partial Solution.** During the loss plateau, the model often has already learned to implement a *partial solution* to the task. This means it correctly predicts a subset of the output tokens, typically those corresponding to an intuitively simpler part of the problem, while failing on the more complex parts. For instance, in the MWS task, the model quickly learns to predict the first output token  $y_1$  correctly (see Figure 2a for the first-token accuracy), as it is simply a copy of the first input token  $x_1$ , while the overall loss remains high and accuracy on subsequent tokens is poor. This ability to solve easier sub-components of the task early on is observed across various algorithmic problems (see Table 1 in Appendix B).

**Repetition Bias.** Concurrent with learning the partial solution, the model’s outputs during the initial phase of training display a strong *repetition bias*, which refers to a tendency of the model to generate repetitive tokens of the form  $x, x, x, \dots$ . One way to quantify such repetitions is to simply count the frequency of output tokens that equal the next one: for output sequence  $y_1, y_2, \dots, y_n$ , define its repetition frequency as,

$$\rho := \frac{1}{n-1} \sum_{i=1}^{n-1} \mathbf{1}[y_i = y_{i+1}].$$

We observe that  $\rho$  increases rapidly during the early phase of training, when the optimal attention map has not been learned yet (Figure 2b). Note that this frequency is small at initialization, and grows rapidly in the first  $\approx 50$  steps to  $\approx 0.8$ , indicating that it is an *implicit bias coming from gradient-based training*.

**Representation Collapse.** Motivated by the frequent repetitions in model outputs, we further study the relation between the hidden representations at different output positions. We find a strong *representation collapse* phenomenon—these representations become nearly parallel in the early phase of training (except for the first output position which is correctly predicted in the partial solution). We measure the pairwise cosine similarity between hidden representations at positions  $i, j$  in the output,

$$\text{COS}_{i,j} := \frac{\langle \mathbf{h}_i, \mathbf{h}_j \rangle}{\|\mathbf{h}_i\| \|\mathbf{h}_j\|}$$

where  $\mathbf{h}_i \in \mathbb{R}^d$  is the hidden state at position  $i$  in the sequence (this quantity is averaged over a random batch of sequences). We find that in the early phase of training, there is a rapid increase in  $\text{COS}_{i,j}$ —averaged over all output positions  $i, j$  except the first position, this quantity increases to  $\approx 0.95$  (Figure 2b). Similar to repetitions, representation collapse is not present at initialization and only appears after a few steps of training. This is in contrast to the *rank collapse* phenomenon for deep softmax-attention Transformers [1] that occurs at initialization. Also, while we focus on the final-layer representation (before the LM layer) in the main text, we show in Figure 28 that representation collapse happens in all intermediate layers to varying degrees.

## 4 The Role of Learning Attention

Observe that though the loss dynamics are abrupt, attention progress measure as well as repetitions and representation collapse are not (Figure 2b); that is, even when the loss is barely decreasing (between steps 50 and 150), attention progress measure notably increases, accompanied by a decrease in repetition frequency and representation collapse. Via training-time interventions, this section shows that learning the attention map plays a crucial role in shaping the loss plateau as well as repetitions and representation collapse.

**Representation Collapse Occurs After the Attention Layer.** We start by verifying whether the attention layer is responsible for representation collapse during the early phase of training. To this end, we plot the cosine similarity of the residual stream for output tokens just before and after the attention layer. Formally, let the residual stream before attention layer (i.e., token + positional embeddings) be  $\mathbf{h}_i \in \mathbb{R}^d$ , and the residual stream after attention layer be  $\mathbf{h}'_i \in \mathbb{R}^d$ , we measure the norm and pairwise cosine similarity for  $\mathbf{h}_i$  and  $\mathbf{h}'_i$  in Figure 27.

We find that in the early phase of training, the cosine similarity between different positions in the post-attention residual stream representations approaches 1.0 rapidly, which is not the case for pre-attention. Furthermore, the norm of  $\mathbf{h}'_i$  grows rapidly in this phase, while the norm of  $\mathbf{h}_i$  remains near-constant. *Hence, in the residual stream, representation collapse occurs after the attention layer during the early phase of training.*

**Biassing the Attention Map.** To study the role of attention map, we slightly modify the training process starting at different time points in training, biassing it towards (or away from) the optimal attention map to check if repetitions, representation collapse, and loss plateau are reduced (resp. amplified).

We do the following: at training time, starting at step  $t_0$ , we multiply the attention map values for output tokens except the first position at  $\Omega$  (i.e. optimal attention map positions) by a constant  $c > 0$ ;

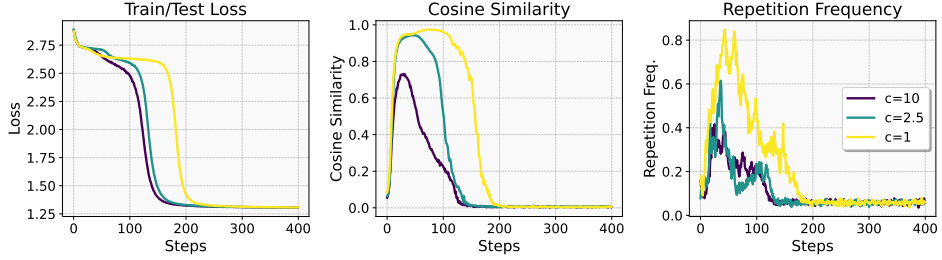


Figure 3: **Biassing attention map by  $c > 1$ .** We find that multiplicative biasing the attention map towards more weight to optimal positions leads to faster convergence, accompanied by less repetitions and average cosine similarity.

for  $c > 1$ , this implies biasing the model towards the final (optimal) attention map, whereas for  $0 < c < 1$ , this implies biasing the model away from the optimal attention map.

We find that, for  $c > 1$  and various values of  $t_0$ , such a scaling leads to lower average cosine similarity between hidden states, lower frequency of repetitions, and faster convergence (Figures 3 and 29). Whereas, for  $0 < c < 1$ , we find the opposite: the model is in representation collapse state for a longer time and converges later compared to the non-scaled ( $c = 1$ ) case, while the repetition frequency remains large throughout the plateau (Figure 4).

For example, for  $t_0 = 0, c = 10$ , i.e. scaling 10 $\times$  from the start of training, we find that the peak cosine similarity attained during training is  $\approx 0.6$ , much smaller than the  $\approx 0.95$  attained for  $c = 1$ , and further the peak for  $c = 10$  is for negligible duration compared to that for  $c = 1$ . Later values of  $t_0 = 25, 50, 75$  show similar results wherein the cosine similarity drops immediately on the above biasing operation, followed by lower repetition frequency and convergence to optimal solution (Figure 29).

On the other hand, for  $t_0 = 0, c = 0.2, 0.5$ , the model takes much longer to converge and is in representation collapse / large repetition frequency state for much longer. This is in line with our expectation that lower attention map values for the optimal positions lead to slower learning and prolonged representation collapse.

*Hence, learning the optimal attention map has a direct effect on shaping the loss dynamics as well as repetitions and representation collapse.*

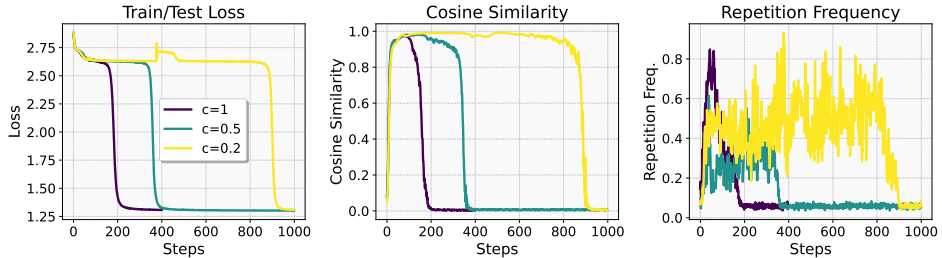


Figure 4: **Biassing attention map by  $c < 1$ .** We find that biasing the attention map to have lesser weight at optimal positions leads to slower convergence, and more representation collapse and repetitions.

**Training with Optimal Attention.** In this test, we initialize with the optimal attention map by fixing embeddings, LayerNorm for attention layer and attention layer weights to their final values at the end of a normal training run, so that at initialization, the correct attention map is already available to subsequent layers. We re-train the subsequent non-fixed layers starting from random initialization.

For the attention layer, we choose the set of parameters to initialize in 2 ways: (a) only Key, Query ( $W_K, W_Q$ ) weights, and (b) All of Key, Query, Value, Output ( $W_K, W_Q, W_V, W_O$ ) weights. We find that in both of these cases, learning only the subsequent layers (i.e. MLP, LM Head) take significantly

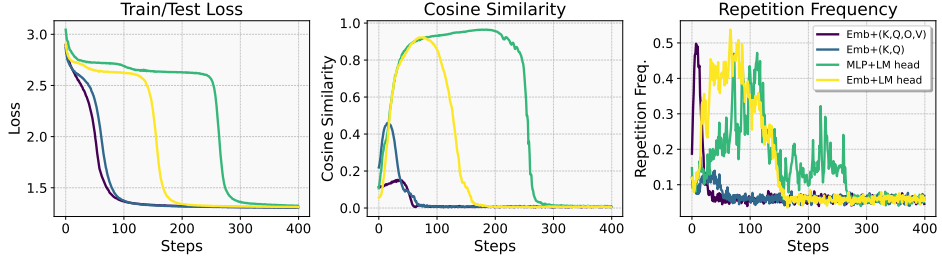


Figure 5: **Different optimal initializations and effect on training.** We find that fixing attention and embedding weights (i.e. attention map) to optimal value, and training other components leads to faster convergence and lesser representation collapse / repetitions. Similar effect does not hold for fixing optimal MLP or Embeddings. ( $K, Q, O, V$  respectively denote the parameters  $W_K, W_Q, W_O, W_V$ .)

shorter time than training the full model, without any significant representation collapse, repetitions or plateau in loss (Figure 5). Further, between (a) and (b), we find that additionally having  $W_O, W_V$  layers initialized to optimal values slightly speeds up learning, and average cosine similarity goes up to approx 0.15 instead of  $\approx 0.45$  when only initializing  $W_K, W_Q$  weights. This indicates that  $W_O, W_V$  layers also play a non-trivial role in causing representation collapse. *This result confirms that attention map is a major bottleneck that leads to early representation collapse and loss plateau.*

**Optimal MLP or Embeddings Do Not Help.** On the other hand, fixing MLP or embeddings (together with LM head) to their final optimal values and re-training the other components does not qualitatively change the training dynamics from the full training case, i.e., a significant loss plateau, repetition bias, and representation collapse still occur (Figure 5). *This indicates that there is little benefit from having the optimal MLP or embeddings at initialization compared to attention map.*

## 5 A Further Look at Repetition Bias

Having observed that Transformer models exhibit a strong repetition bias in the early phase of training, which co-occurs with the loss plateau, we now take a further look at this repetition bias and study how it might be affected by the amount of repetitions in the training sequences. We show that such bias still exists even when there is almost no repetition in the training data. Subsequently, we also show that learning simple, repetitive sequences is easier for Transformers, i.e., no loss plateau, indicating why the model might be biased towards repetitions in the early phase of training.

### 5.1 Beyond Repetitions in Consecutive Tokens

One hypothesis for the reason behind repetition bias is that the training data may consist of some repetitions, and the model may pick up these patterns and amplify them in the early phase of training. To investigate this, we consider a task with low repetitions in the training data. In particular, we consider the *prefix sum* task, where the outputs  $y_1, \dots, y_n$  are defined as  $y_i = (\sum_{j=1}^i x_j) \bmod p$ . Our choice of the input distribution ensures that there is no repetition in consecutive output positions (i.e.,  $y_i \neq y_{i+1}$  for all  $i$ ). Indeed, training a Transformer on the prefix sum task does not result in a significant increase in the repetition frequency at any point in training, unlike the MWS task. Nevertheless, in the early training phase, we still observe that only a few tokens appear repeatedly in the model output though not contiguously as in the MWS task. Therefore, we consider an alternative measure of repetitions based on entropy: for an output sequence  $y_1, y_2, \dots, y_n$ , we define

$$\text{SeqEnt}(y_1, \dots, y_n) := \sum_{i=1}^{|V|} p_i \log(1/p_i); \quad p_i = \frac{|\{y_j = v_i, j \in [n]\}|}{n}$$

i.e. simply the entropy of the empirical distribution of tokens in the sequence. Intuitively, the entropy is lower if most probability mass is concentrated at a few tokens, and larger if the tokens are more uniformly distributed. We find that the model output entropy quickly goes to quite low values early in training compared to the entropy of ground-truth data (Figure 6), indicating that the model still has

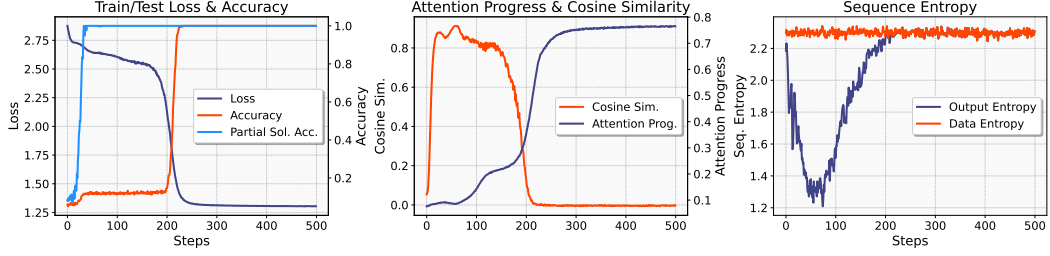


Figure 6: **Prefix sum task training dynamics.** While the usual contiguous repetitions do not occur for this task, an alternate form of repetition occurs in terms of having only a few distinct tokens in the output sequence. ‘Sequence entropy’ quantifies this repetition by measuring the entropy of the empirical distribution of tokens in a sequence, and averaging this entropy over a batch of sequences.

a form of repetition bias. Further, representation collapse still happens in the early phase, with the average cosine similarity going to 0.8 during the plateau.

*Hence, we find that repetition bias might take different forms depending on the task, but still robustly occurs in the early phase of training.*

## 5.2 Repetitive Sequences Are Easier to Learn

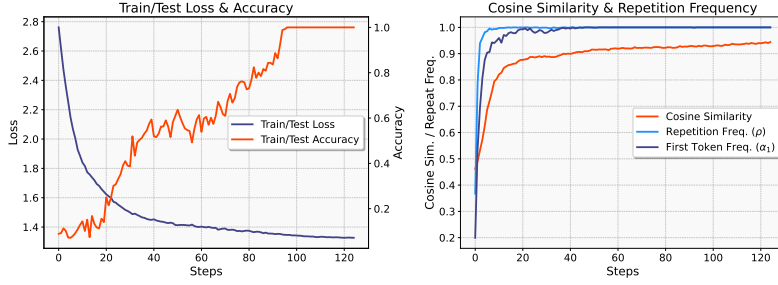


Figure 7: REPEAT<sub>1</sub> training dynamics.

On the other hand, we study what happens when the ground-truth data have a lot of repetitions. We consider a simple task REPEAT<sub>1</sub> of the form  $x_1, x_2, \dots, x_n, \text{SEP}, y_1, y_2, \dots, y_n$ , where  $y_i = x_1 \forall i$ . Unlike other tasks, the loss curve for REPEAT<sub>1</sub> does not have any noticeable plateau, though the accuracy still shows a small plateau period (Figure 7). This observation indicates that such repetitive sequences are easier from an optimization perspective and hence likely “preferred” during the early stage of training. In fact, just one gradient step is sufficient to bring the average representation cosine similarity to  $\approx 0.5$ . We show similar results for other task variants REPEAT<sub>2</sub>, REPEAT<sub>4</sub> in Appendix C.

To further understand the early training phase model output, we define another metric  $\alpha_1$  that measures to what extent the model simply outputs the same token for all output positions:  $\alpha_1 = \frac{1}{n} \sum_{i=1}^n \mathbf{1}[y_i = y_1]$ . Note that this is distinct from accuracy, in that the model might output the wrong  $y_1$ , however repeats  $y_1$  at  $y_2, \dots, y_n$ . We find that  $\alpha_1$  rapidly increases to near perfect values ( $> 0.9$ ) in the early phase of training, showing that the model tends to repeat the first token identically at most positions, even though the output token itself might be incorrect. *Hence, repetitive sequences appear to be inherently easier for the Transformer to learn, and this is likely the reason for repetition bias in the early phase of training.*

## 6 Repetition Bias and Representation Collapse in LLMs

Having established that the degenerate patterns of repetition bias and representation collapse are prevalent in small Transformers trained on algorithmic tasks, a crucial question is whether these phenomena also happen beyond toy settings, specifically during the early pre-training stages of LLMs.

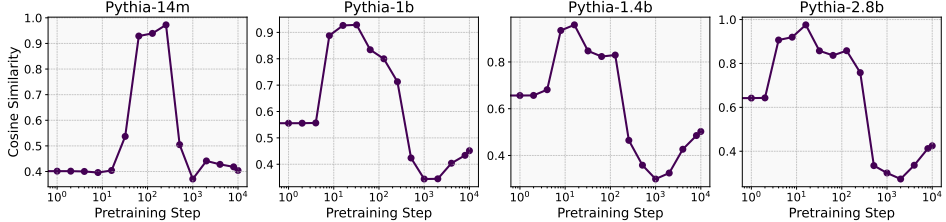


Figure 8: **Representation Collapse during Pythia Pretraining.** Representation collapse at different Pythia pretraining checkpoints; tokens generated via greedy decoding.

We verify that this is indeed the case, using early-stage checkpoints of open-source LLMs Pythia [5] and OLMo-2 [31].

For Pythia models with 14M, 1B, 1.4B, and 2.8B parameters, we find strong representation collapse in the early training steps in their last layers (Figure 8). Specifically, we use 100 questions from the test split of the AI2 ARC-Easy dataset [10]. For each question, we let the model generate 8 tokens, and compute the pairwise cosine similarity of the hidden states (see Appendix A for more implementation details). Figure 8 shows that at initialization, the average cosine similarity is relatively low (0.4-0.65), but within a few steps of training for all models, it sharply increases to  $> 0.9$ . These results remain similar if we use random sampling instead of greedy decoding (Figure 30). Further, the outputs for many prompts in the greedy decoding case are trivial repetitions of the same token, e.g., newline ‘\n’, a clear manifestation of repetition bias.

Similar representation collapse patterns as Pythia are observed for the OLMo-2 7B model. For its earliest available training checkpoint (step 150, OLMo-2-1124-7B), the average representation cosine similarity in the setup from Section 6 is  $\approx 0.93$ ; for the next checkpoint at step 600, this value has already decreased to  $\approx 0.43$  (similar for both greedy decoding and random sampling strategies).

*Hence, repetition bias and representation collapse occur in the early pre-training phase of LLMs, validating our findings beyond toy settings.*

## 7 Related Work

Abrupt learning has been studied in multiple settings; [2] studied it for parity tasks for multiple neural net architectures, while [12] studied abrupt learning for a Markov chain task with Transformers. [15] showed that training a BERT model on matrix completion leads to abrupt learning, while [27] connected abrupt learning for a grammar data setup to graph percolation. For abrupt learning in in-context learning [14], there has been a line of recent works [46, 37, 39, 8, 34, 47] that proposed various theoretical and empirical explanations. We aim to understand a unifying reason behind such observations, in an algorithmic setup for multiple tasks with multi-token output sequences, without restrictive assumptions on our model or training setup.

A line of recent work focused on understanding a related phenomenon of grokking [32], which is abrupt generalization after an extended phase of memorization of training data by the model. Multiple works have studied grokking from the perspective of circuits [30, 38, 29], representation learning [26], delay in feature learning [23, 28, 44], learning syntax for linguistic data [7], and specific properties of softmax attention [17, 33]. We note that grokking is a fixed-dataset phenomenon, while abrupt learning studied in our work is for online training (‘infinite-data’), hence there is no notion of training data memorization. Saddle-to-saddle dynamics [6] have been used to theoretically explain plateaus and sudden drops in loss during training transformers; however, such results require assumptions such as diagonal attention and very small scale of initialization ( $\rightarrow 0$ ). Ideas from statistical physics have also been used towards understanding initial loss plateaus in neural net training [36, 21]; they work in a 2-layer teacher-student neural net setup, where the second layer is fixed during training, and use order parameters to study training. They show that there is a permutation symmetry in the weight vectors of the first layer during the early plateau stage, and exiting this symmetry state is what leads to drop in loss. Another line of work towards understanding stagewise training dynamics of Transformers uses techniques from singular learning theory [19]; the core idea is to estimate the Local Learning Coefficient (LLC) during training, and use this quantity to explain degeneracy in the

loss landscape, and consequently the stage-wise training dynamics of Transformers. The interplay of simplicity bias and Transformer learning dynamics has also been studied recently in [35, 4]. In [4] authors show that neural nets learn to use lower-order moments of data earlier in training, and that the embedding statistics of Transformer models and token  $n$ -gram frequencies are related, explaining a specific distributional simplicity bias during training. [35] show that Transformer-based models progressively learn higher-order (‘many-body’) interactions between tokens in the sequence.

Repetition in language model outputs is a well studied problem [18, 16, 25, 13, 45, 40, 43, 20]. However these works focus not on the early phase of training, but on how repetition may arise in pretrained models, and how to mitigate such phenomena. [9] remarked that in the early phase of training language models, the output might contain some word repetitions, but understanding this occurrence is not the main focus of their work. Rank collapse is a related phenomenon for deep softmax transformers at initialization that might hinder training [1]; however, our representation collapse phenomenon is different in that (i) we use shallow (1 or 2 layers) Transformers instead of deep ones; (ii) we use linear attention instead of softmax; (iii) our observed representation collapse occurs only *after* a few steps of training, not at initialization. Note that we study representation collapse in the early phase of training, which is distinct from the notion of representation collapse in [3]; they show that for 2 sequences  $(v_1, v_2, \dots, v_n)$  and  $(v_1, v_2, \dots, v_n, v_n)$ , as  $n$  grows large, the pretrained model’s hidden state representation for the last token becomes identical for both sequences (Theorem 4.2, [3]).

## 8 Discussion

We identified repetition bias and representation collapse as key characteristics of the early-phase implicit biases of Transformer training, which are closely connected to the commonly observed loss plateau. The question of *why* such degeneracy exists during early time training is an important question for future work. Furthermore, while we showed that the slow rate of learning attention map leads to model remaining in the plateau for an extended time, *why* the rate of learning attention map is slow for algorithmic tasks, and how it connects to the intuitive “complexity” of the task is an interesting question.

**Acknowledgements** PG would like to thank Misha Belkin, Ekdeep Singh Lubana, Yongyi Yang, Zhiwei Xu and Vaibhav Balloli for useful discussions at various stages of this work. Part of this work was done when the authors were visiting the Modern Paradigms in Generalization Program at the Simons Institute for the Theory of Computing.

## References

- [1] Sotiris Anagnostidis, Luca Biggio, Lorenzo Noci, Antonio Orvieto, Sidak Pal Singh, and Aurelien Lucchi. Signal propagation in transformers: Theoretical perspectives and the role of rank collapse. In Alice H. Oh, Alekh Agarwal, Danielle Belgrave, and Kyunghyun Cho, editors, *Advances in Neural Information Processing Systems*, 2022.
- [2] Boaz Barak, Benjamin L. Edelman, Surbhi Goel, Sham M. Kakade, eran malach, and Cyril Zhang. Hidden progress in deep learning: SGD learns parities near the computational limit. In Alice H. Oh, Alekh Agarwal, Danielle Belgrave, and Kyunghyun Cho, editors, *Advances in Neural Information Processing Systems*, 2022.
- [3] Federico Barbero, Andrea Banino, Steven Kapturowski, Dharshan Kumaran, João G. M. Araújo, Alex Vitvitskyi, Razvan Pascanu, and Petar Veličković. Transformers need glasses! information over-squashing in language tasks, 2024.
- [4] Nora Belrose, Quintin Pope, Lucia Quirke, Alex Mallen, and Xiaoli Fern. Neural networks learn statistics of increasing complexity, 2024.
- [5] Stella Biderman, Hailey Schoelkopf, Quentin Gregory Anthony, Herbie Bradley, Kyle O’Brien, Eric Hallahan, Mohammad Aflah Khan, Shivanshu Purohit, USVSN Sai Prashanth, Edward Raff, et al. Pythia: A suite for analyzing large language models across training and scaling. In *International Conference on Machine Learning*, pages 2397–2430. PMLR, 2023.

- [6] Enric Boix-Adsera, Eta Littwin, Emmanuel Abbe, Samy Bengio, and Joshua Susskind. Transformers learn through gradual rank increase, 2023.
- [7] Angelica Chen, Ravid Shwartz-Ziv, Kyunghyun Cho, Matthew L Leavitt, and Naomi Saphra. Sudden drops in the loss: Syntax acquisition, phase transitions, and simplicity bias in MLMs. In *The Twelfth International Conference on Learning Representations*, 2024.
- [8] Siyu Chen, Heejune Sheen, Tianhao Wang, and Zhuoran Yang. Training dynamics of multi-head softmax attention for in-context learning: Emergence, convergence, and optimality, 2024.
- [9] Leshem Choshen, Guy Hacohen, Daphna Weinshall, and Omri Abend. The grammar-learning trajectories of neural language models, 2022.
- [10] Peter Clark, Isaac Cowhey, Oren Etzioni, Tushar Khot, Ashish Sabharwal, Carissa Schoenick, and Oyvind Tafjord. Think you have solved question answering? try arc, the ai2 reasoning challenge. *arXiv:1803.05457v1*, 2018.
- [11] Hugo Cui, Freya Behrens, Florent Krzakala, and Lenka Zdeborová. A phase transition between positional and semantic learning in a solvable model of dot-product attention, 2024.
- [12] Ezra Edelman, Nikolaos Tsilivis, Benjamin L. Edelman, eran malach, and Surbhi Goel. The evolution of statistical induction heads: In-context learning markov chains. In *The Thirty-eighth Annual Conference on Neural Information Processing Systems*, 2024.
- [13] Zihao Fu, Wai Lam, Anthony Man-Cho So, and Bei Shi. A theoretical analysis of the repetition problem in text generation, 2021.
- [14] Shivam Garg, Dimitris Tsipras, Percy Liang, and Gregory Valiant. What can transformers learn in-context? a case study of simple function classes, 2023.
- [15] Pulkit Gopalani, Ekdeep Singh Lubana, and Wei Hu. Abrupt learning in transformers: A case study on matrix completion. In *The Thirty-eighth Annual Conference on Neural Information Processing Systems*, 2024.
- [16] Tatsuya Hiraoka and Kentaro Inui. Repetition neurons: How do language models produce repetitions?, 2025.
- [17] David T. Hoffmann, Simon Schrödi, Jelena Bratulić, Nadine Behrmann, Volker Fischer, and Thomas Brox. Eureka-moments in transformers: Multi-step tasks reveal softmax induced optimization problems, 2024.
- [18] Ari Holtzman, Jan Buys, Li Du, Maxwell Forbes, and Yejin Choi. The curious case of neural text degeneration, 2020.
- [19] Jesse Hoogland, George Wang, Matthew Farrugia-Roberts, Liam Carroll, Susan Wei, and Daniel Murfet. Loss landscape degeneracy drives stagewise development in transformers, 2025.
- [20] M. Emrullah Ildiz, Yixiao Huang, Yingcong Li, Ankit Singh Rawat, and Samet Oymak. From self-attention to markov models: Unveiling the dynamics of generative transformers, 2024.
- [21] Masato Inoue, Hyeyoung Park, and Masato Okada. On-line learning theory of soft committee machines with correlated hidden units –steepest gradient descent and natural gradient descent–. *Journal of the Physical Society of Japan*, 72(4):805–810, April 2003.
- [22] Andrej Karpathy. Karpathy/mingpt: A minimal pytorch re-implementation of the openai gpt (generative pretrained transformer) training, 2022.
- [23] Tanishq Kumar, Blake Bordelon, Samuel J. Gershman, and Cengiz Pehlevan. Grokking as the transition from lazy to rich training dynamics, 2024.
- [24] Nayoung Lee, Kartik Sreenivasan, Jason D. Lee, Kangwook Lee, and Dimitris Papailiopoulos. Teaching arithmetic to small transformers, 2023.

[25] Huayang Li, Tian Lan, Zihao Fu, Deng Cai, Lemao Liu, Nigel Collier, Taro Watanabe, and Yixuan Su. Repetition in repetition out: Towards understanding neural text degeneration from the data perspective. In *Thirty-seventh Conference on Neural Information Processing Systems*, 2023.

[26] Ziming Liu, Ouail Kitouni, Niklas Nolte, Eric J. Michaud, Max Tegmark, and Mike Williams. Towards understanding grokking: An effective theory of representation learning, 2022.

[27] Ekdeep Singh Lubana, Kyogo Kawaguchi, Robert P. Dick, and Hidenori Tanaka. A percolation model of emergence: Analyzing transformers trained on a formal language, 2024.

[28] Kaifeng Lyu, Jikai Jin, Zhiyuan Li, Simon S. Du, Jason D. Lee, and Wei Hu. Dichotomy of early and late phase implicit biases can provably induce grokking, 2024.

[29] William Merrill, Nikolaos Tsilivis, and Aman Shukla. A tale of two circuits: Grokking as competition of sparse and dense subnetworks, 2023.

[30] Neel Nanda, Lawrence Chan, Tom Lieberum, Jess Smith, and Jacob Steinhardt. Progress measures for grokking via mechanistic interpretability. In *The Eleventh International Conference on Learning Representations*, 2023.

[31] Team OLMo, Pete Walsh, Luca Soldaini, Dirk Groeneveld, Kyle Lo, Shane Arora, Akshita Bhagia, Yuling Gu, Shengyi Huang, Matt Jordan, Nathan Lambert, Dustin Schwenk, Oyvind Tafjord, Taira Anderson, David Atkinson, Faeze Brahman, Christopher Clark, Pradeep Dasigi, Nouha Dziri, Michal Guerquin, Hamish Ivison, Pang Wei Koh, Jiacheng Liu, Saumya Malik, William Merrill, Lester James V. Miranda, Jacob Morrison, Tyler Murray, Crystal Nam, Valentina Pyatkin, Aman Rangapur, Michael Schmitz, Sam Skjonsberg, David Wadden, Christopher Wilhelm, Michael Wilson, Luke Zettlemoyer, Ali Farhadi, Noah A. Smith, and Hannaneh Hajishirzi. 2 olmo 2 furious, 2024.

[32] Alethea Power, Yuri Burda, Harri Edwards, Igor Babuschkin, and Vedant Misra. Grokking: Generalization beyond overfitting on small algorithmic datasets. *arXiv preprint arXiv:2201.02177*, 2022.

[33] Lucas Prieto, Melih Barsbey, Pedro A. M. Mediano, and Tolga Birdal. Grokking at the edge of numerical stability, 2025.

[34] Gautam Reddy. The mechanistic basis of data dependence and abrupt learning in an in-context classification task, 2023.

[35] Riccardo Rende, Federica Gerace, Alessandro Laio, and Sebastian Goldt. A distributional simplicity bias in the learning dynamics of transformers, 2025.

[36] David Saad and Sara A. Solla. On-line learning in soft committee machines. *Phys. Rev. E*, 52:4225–4243, Oct 1995.

[37] Aaditya K. Singh, Ted Moskovitz, Felix Hill, Stephanie C. Y. Chan, and Andrew M. Saxe. What needs to go right for an induction head? a mechanistic study of in-context learning circuits and their formation, 2024.

[38] Vikrant Varma, Rohin Shah, Zachary Kenton, János Kramár, and Ramana Kumar. Explaining grokking through circuit efficiency, 2023.

[39] Mingze Wang, Ruoxi Yu, Weinan E, and Lei Wu. How transformers get rich: Approximation and dynamics analysis, 2025.

[40] Weichuan Wang, Zhaoyi Li, Defu Lian, Chen Ma, Linqi Song, and Ying Wei. Mitigating the language mismatch and repetition issues in llm-based machine translation via model editing, 2024.

[41] Jason Wei, Yi Tay, Rishi Bommasani, Colin Raffel, Barret Zoph, Sebastian Borgeaud, Dani Yogatama, Maarten Bosma, Denny Zhou, Donald Metzler, Ed H. Chi, Tatsunori Hashimoto, Oriol Vinyals, Percy Liang, Jeff Dean, and William Fedus. Emergent abilities of large language models. *Transactions on Machine Learning Research*, 2022. Survey Certification.

- [42] Thomas Wolf, Lysandre Debut, Victor Sanh, Julien Chaumond, Clement Delangue, Anthony Moi, Pierrick Cistac, Tim Rault, Rémi Louf, Morgan Funtowicz, Joe Davison, Sam Shleifer, Patrick von Platen, Clara Ma, Yacine Jernite, Julien Plu, Canwen Xu, Teven Le Scao, Sylvain Gugger, Mariama Drame, Quentin Lhoest, and Alexander M. Rush. Huggingface’s transformers: State-of-the-art natural language processing, 2020.
- [43] Jin Xu, Xiaojiang Liu, Jianhao Yan, Deng Cai, Huayang Li, and Jian Li. Learning to break the loop: Analyzing and mitigating repetitions for neural text generation, 2022.
- [44] Zhiwei Xu, Yutong Wang, Spencer Frei, Gal Vardi, and Wei Hu. Benign overfitting and grokking in relu networks for xor cluster data, 2023.
- [45] Junchi Yao, Shu Yang, Jianhua Xu, Lijie Hu, Mengdi Li, and Di Wang. Understanding the repeat curse in large language models from a feature perspective, 2025.
- [46] Yedi Zhang, Aaditya K. Singh, Peter E. Latham, and Andrew Saxe. Training dynamics of in-context learning in linear attention, 2025.
- [47] Nicolas Zucchet, Francesco d’Angelo, Andrew K. Lampinen, and Stephanie C. Y. Chan. The emergence of sparse attention: impact of data distribution and benefits of repetition, 2025.

## A Implementation Details

**Compute Resources.** All experiments were conducted on a single GPU (NVIDIA A100 or L40S) on an academic computing cluster. Most training runs in this paper complete within a few hours.

**Causal Linear Attention.** Linear attention transformer is obtained simply by removing the softmax activation function when computing the attention map, and setting the causal mask to 0 instead of  $-\infty$ . We use the existing minGPT implementation [22] (MIT licence) for our experiments, modifying the code as above and wherever required.

**LLM Experiments.** We use Pythia [5] / OLMo-2 [31] pretrained models (Apache 2.0 Licence) hosted on Huggingface Transformers [42] and run them on the ARC-Easy dataset [10] (CC-BY-SA 4.0 Licence). We set the `use_cache=False` in the `generate` function, and use the hidden state used for predicting each of the 8 output tokens. For random sampling, we use `do_sample=True` (using default temperature value), using `do_sample=False` for our greedy decoding results.

## B Results for Other Algorithmic Tasks

This section presents results on a suite of algorithmic tasks, verifying the generality of our identified phenomena.

Table 1: Algorithmic tasks that show abrupt learning and partial solution during plateau

Task	Description	Partial Solution
Moving Window Sum (MWS)	Sum over moving window of 2 elements, copy 1st element	First input element
Prefix Sum (PRE)	Compute prefix sum of a given $n$ -length sequence	First input element
Permutation (PER)	Permute an $n$ -length sequence by given permutation	Incorrect permutation of input sequence
Multi-Digit Addition (ADD)	Add atmost- $n$ -digit numbers	First digit (0 or 1) i.e. total carry-over from $n$ digits
Histogram (HIST)	Compute counts of each element in $n$ -length sequence	$\approx 100\%$ Repetitive sequences
Reverse (REV)	Reverse $n$ -length input sequence	Repetitive sequences <sup>1</sup>
Copy (COPY)	Copy $n$ -length input sequence	Repetitive sequences <sup>1</sup>

(<sup>1</sup>The loss plateau is very brief, hence a partial solution like other cases is not applicable.)

### B.1 Multi-Digit Addition

This task involves adding 2 atmost 4-digit numbers; if the numbers are represented as  $a = \overline{a_1 a_2 a_3 a_4}$ ,  $b = \overline{b_1 b_2 b_3 b_4}$  and their sum  $a + b = c = \overline{c_0 c_1 c_2 c_3 c_4}$  then the training sequences for ADD are of the form

$$a_1, a_2, a_3, a_4, +, b_1, b_2, b_3, b_4, =, c_4, c_3, c_2, c_1, c_0$$

Note that the output sequence is reversed, following the observations from [24]. We find similar abrupt learning characteristics (Figure 9), partial solution in this case being  $c_0$  i.e. total carry-over from 4 single digit add operations. An interpretable attention map learnt for the output sequence is shown in Figure 10.

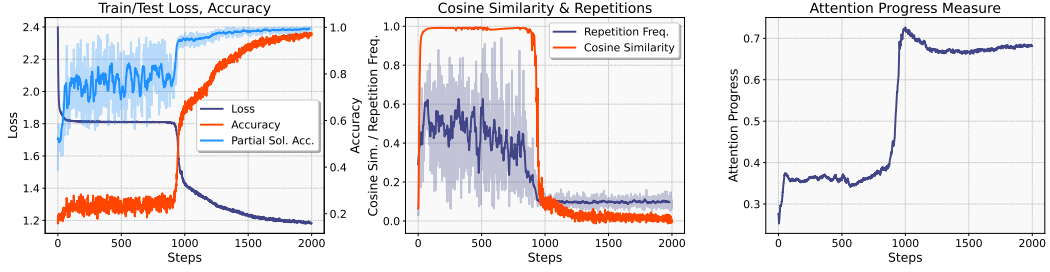


Figure 9: Training dynamics for Add task. (left) Train/Test Loss, Accuracy and Partial solution progress ( $c_0$  accuracy); (middle) Repetition frequency and representation collapse; (right) Attention progress measure.

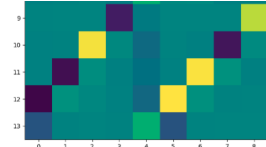


Figure 10: Attention map for add task, note that the model attends to the relevant digits in the input numbers, and to somewhat lesser extent to the preceding digits as well (highlighted positions show entries with larger magnitude).

## B.2 Prefix sum

This task involves computing the cumulative (prefix) sum of an  $n$ -length sequence of integers, so that the training sequences in PRE are of the form ( $n = 16$ , SEP = 17),

$$x_1, x_2, \dots, x_n, \text{SEP}, y_1, y_2, \dots, y_n$$

$$y_i = \left( \sum_{j=1}^i x_j \right) \bmod 17 \quad \forall i \in [n]$$

Training dynamics for this task are shown in Fig. 11 which show similar abrupt learning behavior as MWS and partial solution learning for  $y_1$ . The interpretable attention map learnt for this task is shown in Figure 12.

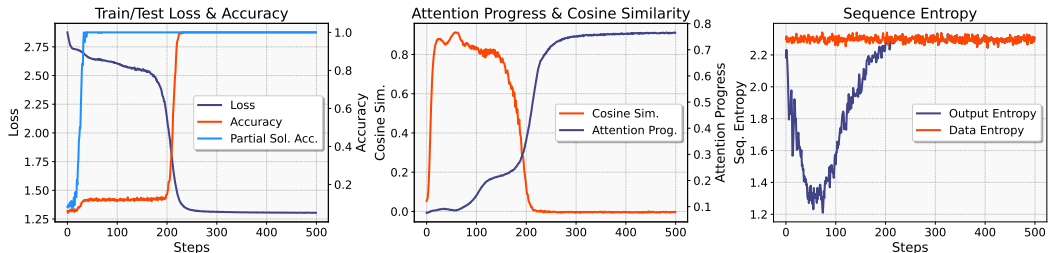


Figure 11: Training dynamics for Prefix sum task. (left) Train/Test Loss, Accuracy and Partial solution progress ( $y_1$  accuracy); (middle) Attention progress and representation collapse; (right) SeqEnt for data and model output sequences.

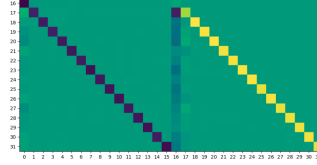


Figure 12: Attention map for Prefix sum task, that uses the relevant token in the input, as well as the previous token in the output to track prefix sum (highlighted positions show entries with larger magnitude).

### B.3 Permutation

This task involves training a 2-layer, 1-head Transformer on permuting a length- $n$  sequence using the permutation  $\pi$ , which is generated at random and is distinct for each training sequence. Formally, for a sequence of positive integers  $(x_1, \dots, x_n)$  and a permutation  $(\pi_1, \dots, \pi_n)$  over  $[n]$ , training sequences for PER,  $k = 0, 1, 2, \dots$  are given by

$$x_1, \dots, x_n, \text{SEP}, \pi_1, \dots, \pi_n, \text{SEP}, x_{\pi_1}, \dots, x_{\pi_n}$$

where  $x_i \sim \text{Unif}\{17, 18, \dots, 32\}$ ,  $n = 16$ ,  $\text{SEP} = 0$ . The partial solution in this case is the output sequence being a permutation of the input sequence  $x_1, \dots, x_n$  i.e., it learns to copy the tokens correctly, but in wrong order (Figure 13). The interpretable attention maps in this case show that the model learns to copy the correct tokens based on the permutation provided (Figure 14a) and then uses them for the final output sequence (Figure 14b).

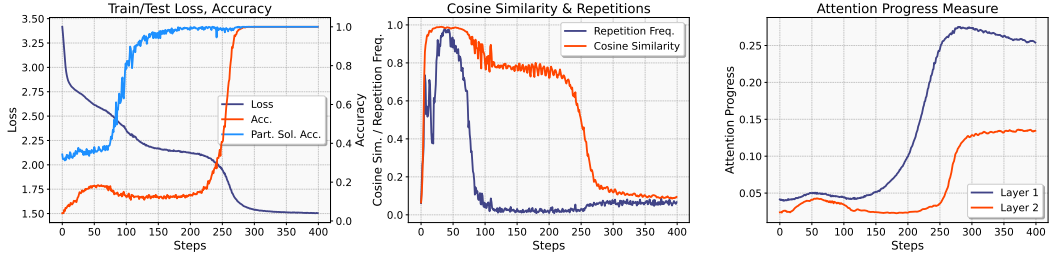
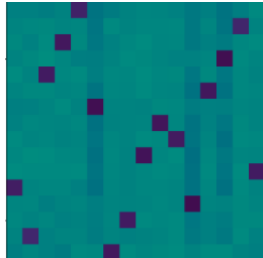
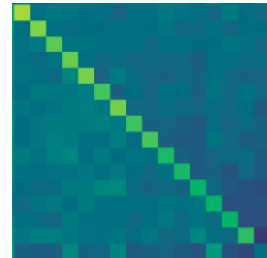


Figure 13: Training dynamics for Permutation task. (left) Train/Test Loss, Accuracy and Partial solution progress; (middle) Repetition frequency and representation collapse; (right) Attention progress measure. Note that the repetition frequency decreases by step 100, which is followed by the partial solution.



(a) Attention map in Layer 1 where rows are attention weights over the input part  $x_1, x_2, \dots, x_n$  of the sequence. The highlighted positions are attending to  $\pi_1, \pi_2, \dots, \pi_n$  = 5, 15, 4, 14, 3, 13, 6, 10, 11, 9, 16, 1, 12, 8, 2, 7. for index  $i \in [n]$ .



(b) Attention map in Layer 2; the rows (output part of the sequence) are attention scores over the part of the sequence to which Layer 1 attention map copies the correctly permuted tokens. This implies that this attention map simply copies the correct token from the residual stream after Layer 1.

Figure 14: Attention maps for the 2 layer Transformer used for Permutation task; highlighted positions show entries with larger magnitude.

## B.4 Histogram

This task [11] involves computing the counts of elements in the input sequence, and training sequences are of the form

$$x_1, x_2, \dots, x_n, \text{SEP}, y_1, y_2, \dots, y_n$$

$$y_i = \sum_{j=1}^n \mathbf{1}[x_j = x_i]$$

where  $x_i \sim \text{Unif}\{1, 2, \dots, 12\}$ ,  $n = 16$ ,  $\text{SEP} = 0$ . We train a 2-layer, 1-head transformer for this task, with gradient clipping (1.0) to avoid loss spikes (Figure 15). We note that the repetition bias in this case is quite strong which leads to  $\approx 100\%$  repetitions in the early phase of training, and which we characterize as partial solution for this task. Further we only consider the attention map from layer 1 Figure 16 since this is the most consistent and clearly interpretable across runs, and indicates an identity-map-like function.

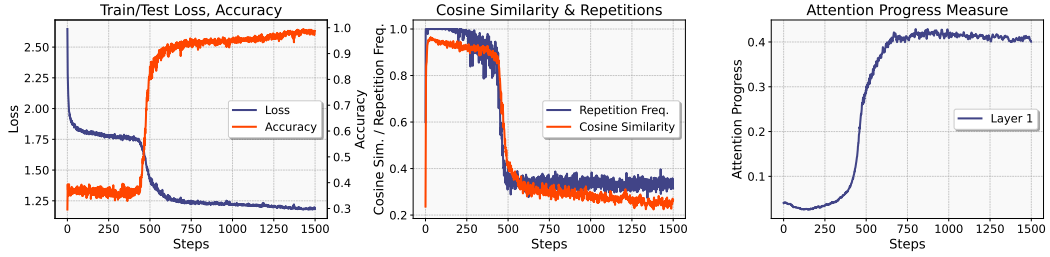


Figure 15: Training dynamics for Histogram task. (left) Train/Test Loss and Accuracy; (middle) Repetition frequency and representation collapse; (right) Attention progress measure. We only measure attention progress for the 1st layer, since that is the one that consistently and clearly shows an interpretable pattern (Figure 16).



Figure 16: Attention map in layer 1 for histogram task, where rows for the latter half of the sequence compute attention weights over the input tokens  $x_i$ , similar to an identity map (highlighted positions show entries with larger magnitude).

## B.5 Reverse

This is the task of reversing the input sequence, so that the training sequences for reverse task REV are given as,

$$x_1, x_2, \dots, x_n, \text{SEP}, x_n, x_{n-1}, \dots, x_1$$

for  $x_i \sim \text{Unif}\{1, 2, \dots, 16\}$ ,  $n = 16$ ,  $\text{SEP} = 0$ . The training dynamics are shown in Figure 17a and the interpretable attention map is shown in Figure 17b.

## B.6 Copy

This is the trivial task of copying the input sequence as is, so that the training sequences for copy task COPY are given as,

$$x_1, x_2, \dots, x_n, \text{SEP}, x_1, x_2, \dots, x_n$$

for  $x_i \sim \text{Unif}\{1, 2, \dots, 16\}$ ,  $n = 16$ ,  $\text{SEP} = 0$ . The training dynamics are shown in Figure 18a and the interpretable attention map is shown in Figure 18b.

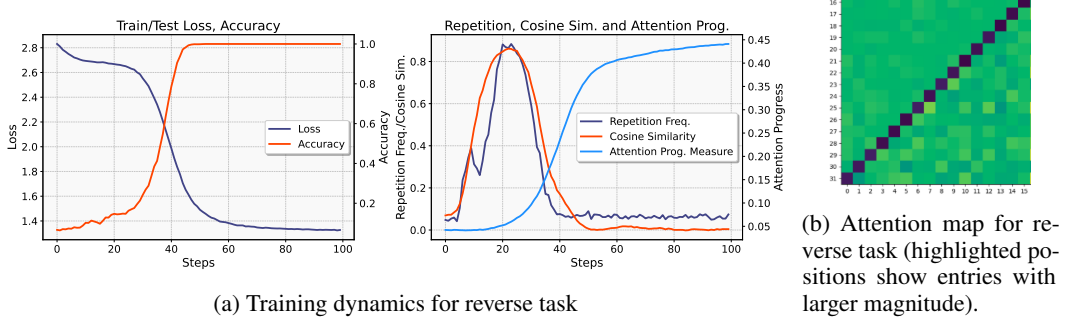


Figure 17: **Training dynamics for Reverse task.** We see Abrupt Learning, Representation Collapse and Repetitions, though to a lesser extent than MWS task. Note that the plateau is much shorter compared to MWS, possibly explained by the fact that reversing a sequence is ‘easier’ than computing the moving window sum.

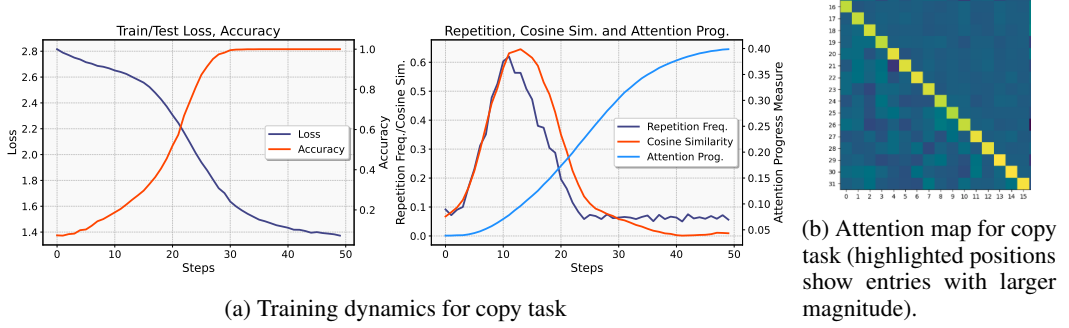


Figure 18: **Training dynamics for Copy task.** Similar to reverse task, we observe Abrupt Learning, Representation Collapse and Repetitions for Copy task, but this time to an even lesser extent than reverse task itself.

## C Results for REPEAT<sub>2</sub> and REPEAT<sub>4</sub>

**REPEAT<sub>2</sub>** This task is defined as,

$$y_i = \begin{cases} x_1 & 1 \leq i \leq 8 \\ (x_1 + 1) \bmod 17 & 9 \leq i \leq 16 \end{cases}$$

The training dynamics for REPEAT<sub>2</sub> are given in Figure 19a. We find that similar to REPEAT<sub>1</sub>, the training loss does not exhibit any plateau. Moreover, the repetition frequency  $\rho$  and metric  $\alpha_1$  increase rapidly to  $\approx 1.0$  early on in training. We measure the average cosine similarity for hidden states for repetitive blocks of the output sequence (see Figure 19b).

**REPEAT<sub>4</sub>** This task is defined as

$$y_i = \begin{cases} x_1 & 1 \leq i \leq 4 \\ (x_1 + 1) \bmod 17 & 5 \leq i \leq 8 \\ (x_1 + 2) \bmod 17 & 9 \leq i \leq 12 \\ (x_1 + 3) \bmod 17 & 13 \leq i \leq 16 \end{cases}$$

Similar results are observed for REPEAT<sub>4</sub> as well; for this case we measure the average cosine similarity for hidden states for repetitive blocks of the output sequence (see Figure 20b).

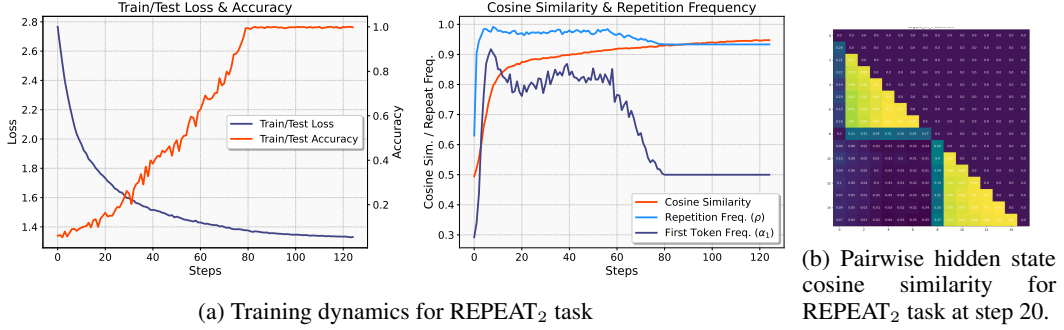


Figure 19: **REPEAT<sub>2</sub> training dynamics.** Note that there is no plateau in loss, similar to the REPEAT<sub>1</sub> task. Further, the pairwise cosine similarity for hidden states take a specific form indicating the blocks of repeated tokens in the output.

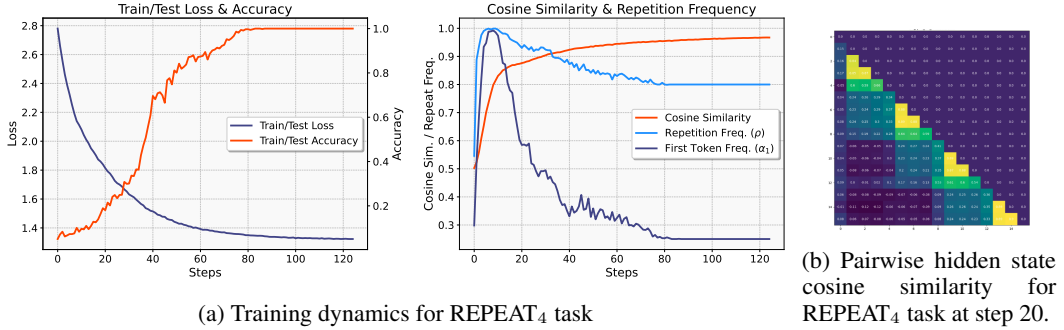


Figure 20: **REPEAT<sub>4</sub> training dynamics.** Similar to REPEAT<sub>2</sub>, there is no plateau in loss. The pairwise cosine similarity for hidden states takes a form indicating the blocks of repeated tokens in the output.

## D Varying Configurations

We demonstrate below that abrupt learning, representation collapse and repetition bias occur across model hyperparameter variations for the MWS task (Figures 21 to 25). We also show that training using SGD instead of Adam also demonstrates similar abrupt learning characteristics (Figure 26).

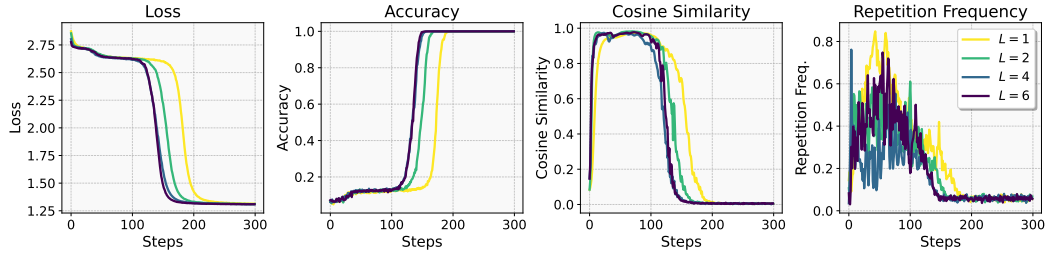


Figure 21: **Number of Layers (L).** We show that abrupt learning, representation collapse in the last layer and repetitions occur for multi (2, 4, 6)-layer models as well.

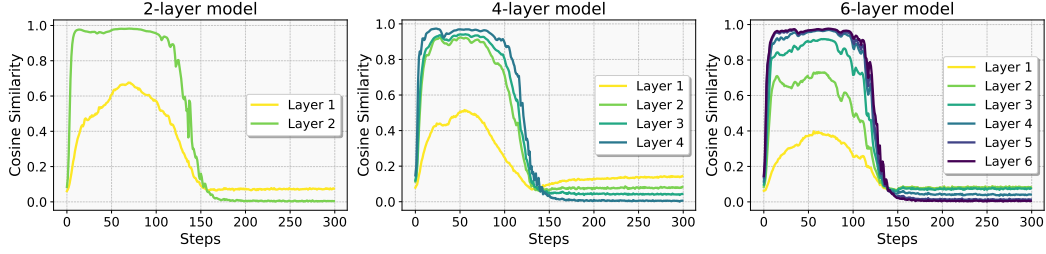


Figure 22: **Extent of Representation collapse at various intermediate layers.** Cosine similarity values showing the extent of representation collapse after each intermediate layer in multi-layer models. Note that the representation collapse is not so severe in the early layers of multi-layer models, but the cosine similarity becomes close to 1.0 as we progress to the final layer.

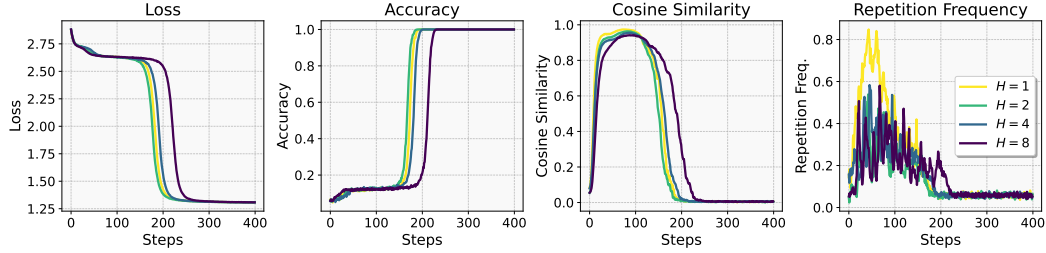


Figure 23: **Number of attention heads ( $H$ ).** We show that abrupt learning with representation collapse and repetition bias occurs in 1-layer multi-attention head models as well.

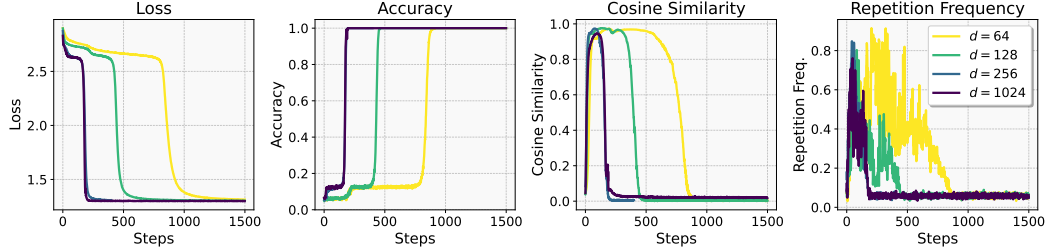


Figure 24: **Embedding dimension ( $d$ ).** We show that abrupt learning with representation collapse and repetition bias occurs in 1-layer 1-head models with different embedding dimension. Note that the convergence is delayed for models with smaller values of  $d = 64, 128$ .

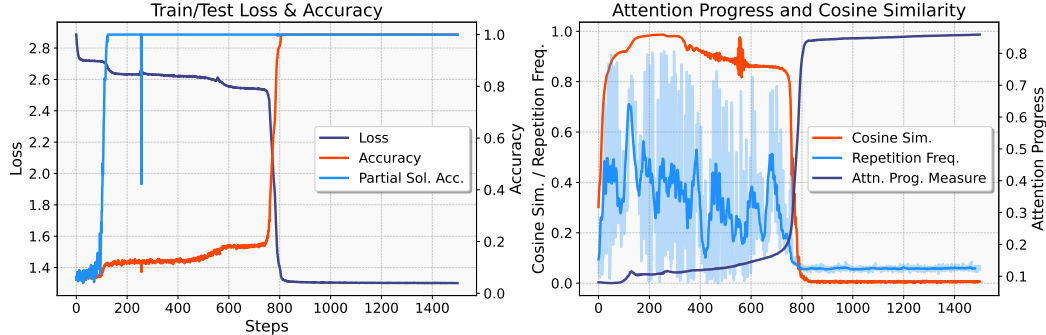


Figure 25: **Softmax Attention.** For completeness we show that repetition bias and early-phase representation collapse are not limited to linear transformers but are observed in softmax attention transformers as well. Note that the loss plateau is longer than that for linear attention.

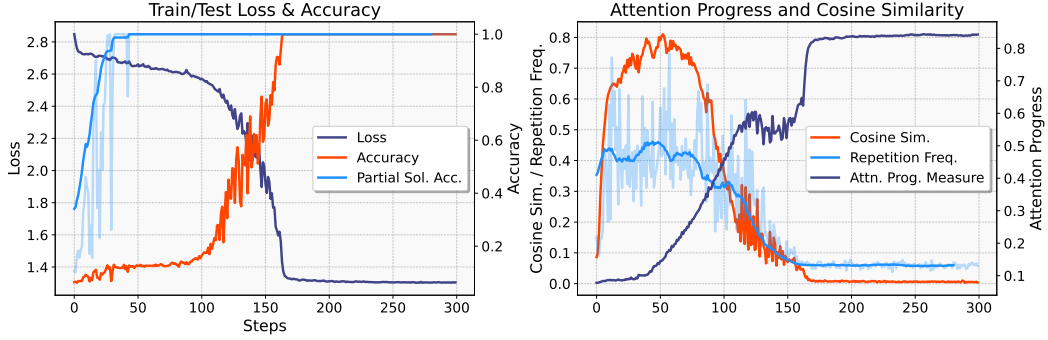


Figure 26: **SGD instead of Adam for loss optimization.** We show that abrupt learning is not limited to Adam optimizer, and occurs with SGD ( $\eta = 0.1$ ) as well. We chose this value of  $\eta$  since smaller values typically lead to much longer periods of little decrease in loss, without increase in accuracy.

## E Additional Figures

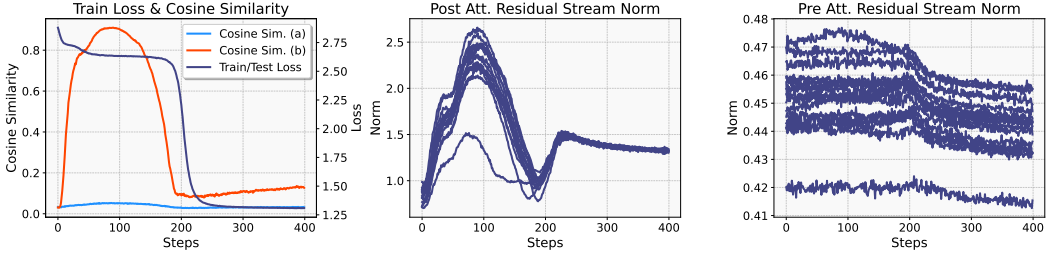


Figure 27: Norm and representation collapse dynamics for (a) pre- and (b) post-attention residual streams for all positions  $i, j$  except the first position.

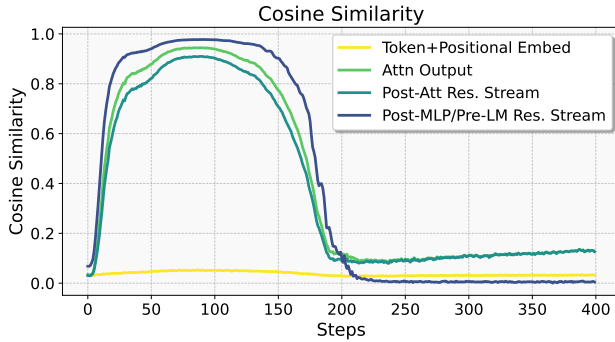


Figure 28: Cosine similarity at various points in residual stream for 1-layer, 1-head Transformer trained on MWS task.

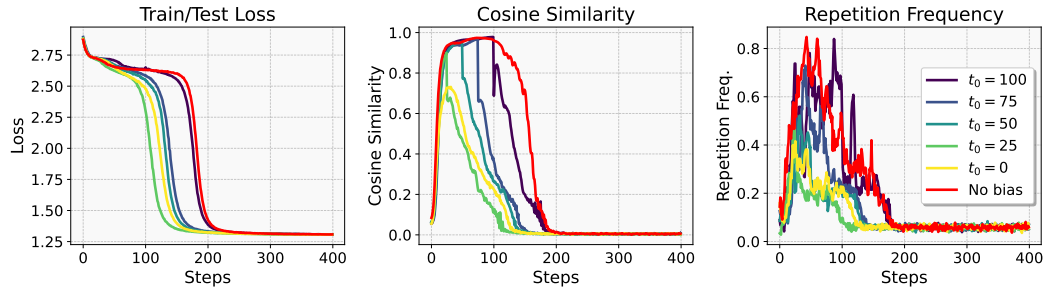


Figure 29: Biasing attention map by  $c = 10$  at different  $t_0$  during training.

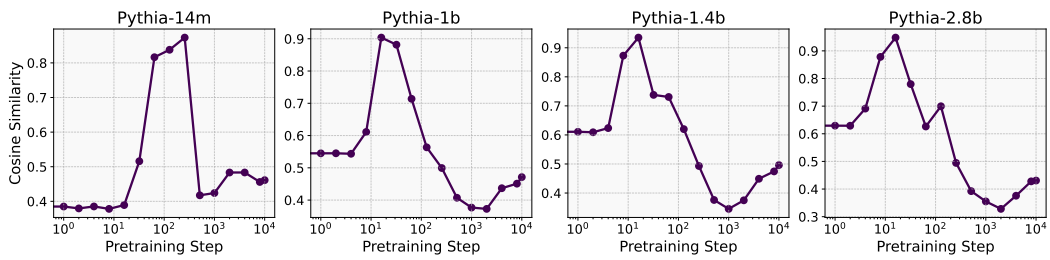


Figure 30: Representation collapse at different Pythia pretraining checkpoints; inference with random sampling.